Identification of Dynamic Model Parameters for Lithium-Ion Batteries used in Hybrid Electric Vehicles

Caiping Zhang[1], Jiazhong Liu[2], S.M.Sharkh[2], Chengning Zhang[1]

(1. National Engineering Laboratory for Electric vehicle, School of Mechanical and Vehicular Engineering, Beijing Institute of Technology, Beijing 100081, China;
2. School of Engineering Sciences, University of Southampton, Highfield, Southampton, SO17 1BJ, UK)

Abstract: This paper presents an electrical equivalent circuit model for lithium-ion batteries used for hybrid electric vehicles (HEV). The model has two RC networks characterizing battery activation and concentration polarization process. The parameters of the model are identified using combined experimental and Extended Kalman Filter (EKF) recursive methods. The open-circuit voltage and ohmic resistance of the battery are directly measured and calculated from experimental measurements, respectively. The rest of the coupled dynamic parameters, i.e. the RC network parameters, are estimated using the EKF method. Experimental and simulation results are presented to demonstrate the efficacy of the proposed circuit model and parameter identification techniques for simulating battery dynamics.

Keywords: Parameters identification; dynamic battery model; lithium-ion battery; HEV;

CLC number: TM912.8 **Document code**: A **Article ID**:

1. Introduction

Lithium-ion batteries are increasingly used in portable electronics, automotive and aerospace applications, as well as in back-up power applications due to their high voltage, high energy density, none memory effect, and low self-discharge during storage. Recently there has been a fast growth in demand for large lithium-ion batteries for direct power supply of electric vehicles (EV) and hybrid electric vehicles (HEVs). Accurate modeling of battery dynamics is important for accurate simulation and optimization, and real time energy management of EVs and HEVs.

An accurate dynamic model of battery usually involves the relations of the terminal voltage to current, power, temperature, state of charge (SOC), the effects of self-discharge, and the effects of aging. Currently, there are three main types of model used to describe the relationship between input and output of a battery system. These are electrochemical model [1, 2], artificial neural network model [3, 4] and electrical equivalent circuit model [5-7]. The electrochemical battery model describes the dynamic process of chemical reactions occurring on the electrodes based on mathematical method, which can integrally reflect dynamic characteristics of the battery. However, this model requires battery chemical parameters and detailed knowledge of the battery construction and material properties which is not normally available to designers of vehicles.

The artificial neural networks method has advantage of adaptive learning which can be applied to the system identification of battery's nonlinear characteristics during charging and discharging. The artificial neural networks model has be widely implemented for various battery systems. However, this model requires a large amount of data for training and the accuracy of these models

is affected significantly by the training data and training method. Furthermore, the neural network model may not be suitable for simulating battery characteristics of HEV since the battery current fluctuates acutely and randomly as the power demand varies during a vehicle's driving cycles.

Electrical equivalent circuit models are based on the operational principle of the battery which simulates its dynamics with circuit network composed of capacitor, resistor, and constant voltage source etc. Equivalent circuit models have been extensively researched in recent years due to its excellent adaptability and simple realization. Several equivalent circuit models such as RC model, Thevenin model and Partnership for a New Generation of Vehicles (PNGV) model have been applied to lithium-ion batteries in HEV. These models are used for simulating the dynamic characteristics and estimating SOC of the battery.

The parameters of equivalent circuit model for batteries are normally determined by performing a series of charging and discharging tests at different SOC values with controlled current and temperature. Various techniques have been proposed to identify the model parameters.. For example, the identification technique, based on experimental data coupled with characteristics of battery model, is essentially utilized for specifying the parameters [8, 9]. However, it requires highly accurate measurement apparatus to obtain the resistance and time constant of RC network in the model. In addition, it heavily relies on the experience of the researcher. The well known Extended Kalman Filter (EKF) is a recursive algorithm for computing estimates of states and parameters of nonlinear system. It is particularly able to optimally estimate the states and parameters affected by process and measurement noise [10]. It has been applied in a wide range of applications such as state observation, parameter estimation and state prediction problems. In this paper, the EKF combined with the experimental identification methods are used to obtain the circuit model parameters of a lithium ion battery.

2. Model formulation

The power assist unit in the hybrid electric vehicle described in this paper, is composed of 144 lithium-ion cells. Each battery module (battery box) consists of 16 lithium-ion cells. Ideally, tests and model identification need to be carried out on each cell with a large quantity of computation. But this will be expensive and time consuming. Alternatively, tests and modelling could be based on one cell, and then multiply by144 to obtain a model of the whole battery pack. But this may not be accurate due to tolerance variations between the battery cells. As a compromise the battery module of 16 cells is regarded as the object for modelling, multiplying the amount of battery modules as the total battery pack model.

The electrical circuit model is used to describe the relationship between the currents and voltages measured at the terminal of the battery. The model used for the lithium-ion battery comprises three parts, as shown in Fig. 1: 1) open-circuit battery voltage V_{oc}, which is composed of an equilibrium potential V_e and a hysteresis voltage V_h, 2) internal resistance R_i contains the ohmic resistance R_o and the polarization resistance, where the polarization resistance has two components R_{pa} and R_{pc}, where R_{pa} represents effective resistance characterising activation polarization and R_{pc} represents effective resistance characterising concentration polarization, 3) effective

capacitances, which consists two parameters of C_{pa} and C_{pc}, these two parameters are used to describe the activation polarization and concentration polarization, which are used to characterise the transient response during transferring power to/from the battery. The electrical behaviour of the circuit can be expressed as following equations:

$$\dot{V}_{pa} = -\frac{V_{pa}}{R_{pa}C_{pa}} + \frac{I}{C_{pa}} \tag{1}$$

$$\dot{V}_{pc} = -\frac{V_{pc}}{R_{pc}C_{pc}} + \frac{I}{C_{pc}} \tag{2}$$

$$V_L = V_e + V_h - V_{pa} - V_{pc} - IR_o \tag{3}$$

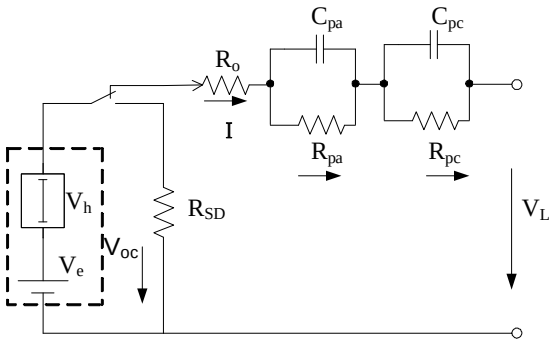

Fig. 1 Proposed equivalent circuit model for the lithium-ion battery

3. Parameters estimation

3.1 Open-circuit voltage

The equilibrium potential is the open circuit voltage measured when the forward and reverse reaction rates are equal in an electrolytic solution, thereby establishing the potential of an electrode. The equilibrium potential of the battery, which is determined by Nernst equation, depends on the temperature and the amount of active material left in the electrolyte. Fig. 2 illustrates the open-circuit voltage (OCV) as a function of SOC after charge and discharge at room temperature. In this experiment, the battery was first discharged at constant current of 30 A from fully charged state till 10 % of the nominal capacity (100 A h) was consumed. It was subsequently left in open-circuit condition, while the open-circuit voltage was observed. After one hour, the measured voltage was considered as equilibrium voltage since the rate of the increase of the open circuit voltage was negligible and hence the battery was assumed to be got to a steady state. The battery was subsequently discharged by a further 10 % of the nominal at the same current and the equilibrium voltage measured after waiting for one hour, and the procedure was repeated to obtain the remaining data points on the discharge curve in Fig. 2. The battery was then recharged at the specified current, the equilibrium voltage after charge could be obtained every 0.1 SOC. From Fig. 2, we can find that the equilibrium voltage has different values after charge and discharge

respectively at the same SOC, which indicates that the equilibrium potential depends on previous treatment of the battery and the hysteresis phenomenon is observed during a charge and discharge. Thus, two SOC values exist for a given equilibrium voltage. The hysteresis voltage needs to be considered when the open-circuit voltage is used to determine a battery's initial SOC.The hysteresis characteristics is thought to be due to the intercalation of lithium ions into carbon and into $LiMnO_2$ electrodes for lithium-ion batteries as discussed in [11-14].

In this paper, in order to identify the model parameters, we assume SOC point is known. Hysteresis will be neglected and the average open-circuit voltage of battery V_{oc} will be used.

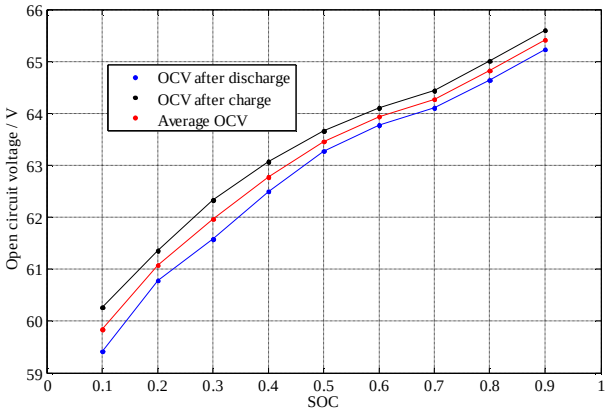

Fig. 2 Open-circuit of battery voltage as a function of SOC at room temperature

3.2 Ohmic resistance

The total Ohmic impedance of the battery is the sum of the resistance across the solution and the resistance of the external circuit, which depend on temperature and SOC. The Ohmic resistance of the battery at the specified SOC and temperature can be determined experimentally using pulse current charging and discharging as illustrated in Fig. 3.

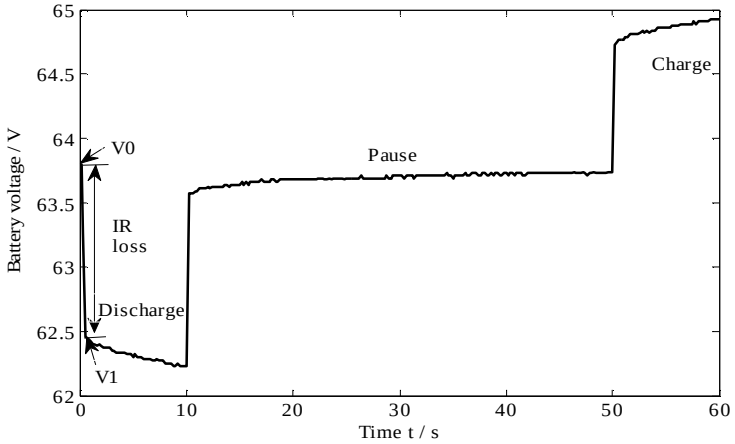

Fig. 3 Battery voltage response at the pulse current

As shown in Fig. 3, the instantaneous battery voltage is dropped at the condition of pulse current which can be expressed as:

$$\Delta V = |V_1 - V_0| \tag{4}$$

The ohmic resistance can be given by:

$$R_o = \frac{\Delta V}{|I|} \tag{5}$$

Where I is the charge/discharge current through the battery.

The Ohmic resistance was found to be independent of the battery current. But it was found to be a function of SOC shown in Fig. 4. It can be seen that the resistance varies with SOC, and has high values at lower SOC and also has a high value at SOC=1.

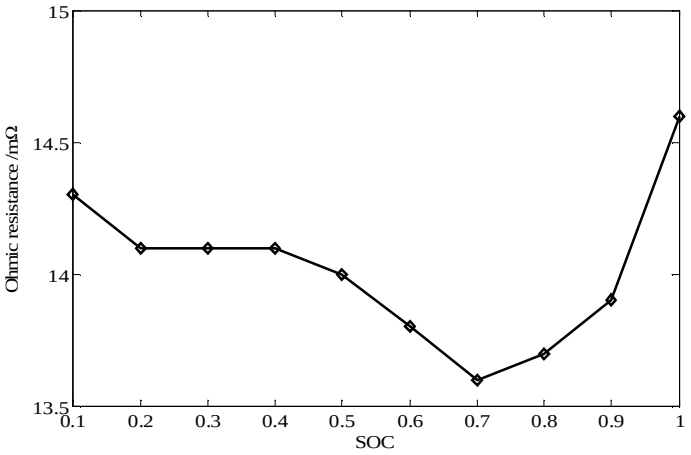

Fig. 4 Ohmic resistance of the battery as a function of SOC at room temperature

3.3 Identification of dynamic behaviour parameters

3.3.1 The extended Kalman filter

The Kalman filter is a mathematical technique that provides an efficient recursive means for estimating the states of a process, in such a way so as to minimize the mean of the squared error [15]. The filter has been applied extensively to the field of linear estimation including state estimation, parameters estimation and dual estimation. The extended Kalman filter (EKF) is a nonlinear version of Kalman filter that linearizes about the current mean and covariance of the state. It can be described as follows [16]: the system of interest is continuous-time dynamics with discrete-time measurements given by:

$$\begin{aligned} \dot{x} &= f(x, u, w, t) \\ y_k &= h_k(x_k, v_k) \\ w(t) &\sim (0, Q) \\ v_k &\sim (0, R_k) \end{aligned} \tag{6}$$

where $u(t)$ is the control input; $w(t)$ represents process noise which is assumed to be continuous-time Gaussian zero-mean white noise with covariance of Q ; v_k represents measurement noise which is assumed to be discrete-time Gaussian white noise with zero mean and a covariance R_k . The procedure for using the EKF for optimal state and parameter estimation can

be summarised as follows:

Step *I* : Initialisation

The initial estimation of x_0 before any measurement is modelled as a Gaussian random vector with mean X_0 and covariance P_0, which is expressed by:

$$\begin{aligned} \hat{x}_0^+ &= E[x_0] \\ P_0^+ &= E[(x_0 - \hat{x}_0^+)(x_0 - \hat{x}_0^+)^T] \end{aligned} \tag{7}$$

Step *II*: time update (from time $(k-1)^+$ to time $(k)^-$)

The time update phase uses the state estimate and its covariance from the previous time step $(k-1)^+$ to produce an estimate of the state at the current time step $(k)^-$ as follows:

$$\begin{aligned} \dot{\hat{x}} &= f(\hat{x}, u, 0, t) \\ \dot{P} &= AP + PA^T + Q \end{aligned} \tag{8}$$

Where A is a partial derivate Jacobian matrix evaluated at the current state estimate which can be given as:

$$A = \left.\frac{\partial f}{\partial x}\right|_{x=\hat{x}} \tag{9}$$

In this step, the integration is processed with $\hat{x} = \hat{x}_{k-1}^+$ and $P = P_{k-1}^+$. At the end of the integration, we have $\hat{x} = \hat{x}_k^-$ and $P = P_k^-$. With reference to equation (8), the estimated state and its covariance propagates from time $(k-1)^+$ to time $(k)^-$ based on the previous values, system dynamics, the control input and the errors of the actual system [17].

Step *III*: measurement update

In this phase, the measurement information at time k is processed to refine the estimate of x_k to arrive at a more accurate state estimate. The resulting estimate of x_k is denoted $\hat{x}_k^+$, and its covariance is denoted P_k^+. Performing the measurement update of the state estimate and estimation error covariance, the measurement update equation can be described as follows:

$$\begin{aligned} K_k &= P_k^- C_k^T (C_k P_k^- C_k^T + R_k)^{-1} \\ \hat{x}_k^+ &= \hat{x}_k^- + K_k (y_k - h_k(\hat{x}_k^-, 0, t_k)) \\ P_k^+ &= (I - K_k C_k) P_k^- (I - K_k C_k)^T + K_k R_k K_k^T \end{aligned} \tag{10}$$

Where K_k is Kalman gain matrix; C_k is the partial derivative of $h_k(x_k, v_k)$ with respect to x_k, which is given by:

$$C_k = \left.\frac{\partial h}{\partial x}\right|_{x=\hat{x}_k^-} \tag{11}$$

It should be noted that $\hat{x}_k^-$ and $\hat{x}_k^+$ are both estimates of the same quantity; and are both estimates of x_k. However, $\hat{x}_k^-$ is the estimate of x_k *before* the measurement y_k is taken into account, which is called *priori* estimate, and $\hat{x}_k^+$ is the estimate of *after* the measurement y_k is taken into account, which is called *posteriori* estimate.

3.3.2 Implementation

This section presents the implementation for estimating states and parameters of the dynamic battery model. For the electrical circuit model, the output voltage of the battery is based on equation (3) which can be rearranged by

$$V_L = V_{oc} + [-1 \quad -1]\begin{bmatrix} V_{pa} \\ V_{pc} \end{bmatrix} - [R_o]I \tag{12}$$

where V_{oc} represents the average voltage of the battery open-circuit voltage. The current flowing out of the battery is assumed positive for this study.

Taking time derivative of output voltage of the battery and assuming $dV_{oc}/dt \approx 0$, $dI/dt \approx 0$ (the rate of change of open-circuit voltage and terminal current between sampling time is negligible) gives:

$$\dot{V}_L = \left[-\frac{1}{R_{pc}C_{pc}}\right]V_L + \left[\frac{1}{R_{pa}C_{pa}} - \frac{1}{R_{pc}C_{pc}}\right]V_{pa} - \left[\frac{R_o}{R_{pc}C_{pc}} + \frac{1}{C_{pc}} + \frac{1}{C_{pa}}\right]I + \left[\frac{1}{R_{pc}C_{pc}}\right]V_{oc} \tag{13}$$

In this study, the parameters R_{pa}, C_{pa}, R_{pc}, C_{pc} are considered as constant at a specified SOC.

The parameters considered as states are added to the state variables. Combing equations (1), (2), (12) and (13), the system can be expressed as follows:

$$\begin{aligned} \dot{x}_k &= f(x,u) \\ y_k &= h_k(x_k) \end{aligned} \tag{14}$$

where $x = [V_{pa} \quad V_{pc} \quad V_L \quad \frac{1}{R_{pa}} \quad \frac{1}{C_{pa}} \quad \frac{1}{R_{pc}} \quad \frac{1}{C_{pc}}]^T$,

$u = I$, $h_k(x_k) = V_{Lk}$.

$f(x,u) = [f_1 \quad f_2 \quad f_3 \quad f_4 \quad f_5 \quad f_6 \quad f_7]^T$

and $f_1 = -x_1x_4x_5 + x_5u$;

$f_2 = -x_2x_6x_7 + x_7u$;

$f_3 = -x_6x_7x_3 + (x_4x_5 - x_6x_7)x_1 - (R_ox_6x_7 + x_5 + x_7)u + x_6x_7V_{oc}$;

$f_4 = 0$; $f_5 = 0$; $f_6 = 0$; $f_7 = 0$.

Then we can calculate the matrices of the system by

$$A = \left.\frac{\partial f}{\partial x}\right|_{x=\hat{x}} = \begin{bmatrix} a_{11} & 0 & 0 & a_{14} & a_{15} & 0 & 0 \\ 0 & a_{22} & 0 & 0 & 0 & a_{26} & a_{27} \\ a_{31} & 0 & a_{33} & a_{34} & a_{35} & a_{36} & a_{37} \\ 0 & 0 & 0 & 0 & 0 & 0 & 0 \\ 0 & 0 & 0 & 0 & 0 & 0 & 0 \\ 0 & 0 & 0 & 0 & 0 & 0 & 0 \\ 0 & 0 & 0 & 0 & 0 & 0 & 0 \end{bmatrix}$$

Where

$$a_{11} = -x_4 x_5, \quad a_{14} = -x_1 x_5, \quad a_{15} = -x_1 x_4 + u$$
$$a_{22} = -x_6 x_7, \quad a_{26} = -x_2 x_7, \quad a_{27} = -x_2 x_6 + u$$
$$a_{31} = x_4 x_5 - x_6 x_7, \quad a_{33} = -x_6 x_7, \quad a_{34} = x_5 x_1, \quad a_{35} = x_4 x_1 - u,$$
$$a_{36} = -x_7 x_3 - x_7 x_1 - R_o x_7 u + V_{oc} x_7, \quad a_{37} = -x_6 x_3 - x_6 x_1 - R_o x_6 u - u + V_{oc} x_6.$$

$$C = [0 \quad 0 \quad 1 \quad 0 \quad 0 \quad 0 \quad 0]$$

Fig. 5 shows the estimating results with EKF algorithm for the states and parameters of the model at the point of 100 % SOC. In this case, the covariance matrices Q, P_0 and R selected are given by:

$$Q = \begin{bmatrix} 0.00001 & 0 & 0 & 0 & 0 & 0 & 0 \\ 0 & 0.00001 & 0 & 0 & 0 & 0 & 0 \\ 0 & 0 & 0.00001 & 0 & 0 & 0 & 0 \\ 0 & 0 & 0 & 0.00001 & 0 & 0 & 0 \\ 0 & 0 & 0 & 0 & 0.00001 & 0 & 0 \\ 0 & 0 & 0 & 0 & 0 & 0.00001 & 0 \\ 0 & 0 & 0 & 0 & 0 & 0 & 0.00001 \end{bmatrix},$$

$$P_0 = \begin{bmatrix} 0 & 0 & 0 & 0 & 0 & 0 & 0 \\ 0 & 0 & 0 & 0 & 0 & 0 & 0 \\ 0 & 0 & 1000 & 0 & 0 & 0 & 0 \\ 0 & 0 & 0 & 20 & 0 & 0 & 0 \\ 0 & 0 & 0 & 0 & 10\mathbf{E}-6 & 0 & 0 \\ 0 & 0 & 0 & 0 & 0 & 10\mathbf{E}7 & 0 \\ 0 & 0 & 0 & 0 & 0 & 0 & 10\mathbf{E}-4 \end{bmatrix},$$

$$R = 10.$$

Fig. 5 (a) and (b) shows the behaviour of the estimated voltages characterising battery polarizations. Fig. 5 (a) shows that the voltage of capacity characterising battery activation polarization reaches steady-state within 4 seconds, which suggests that time constant of the RC network is small. However, the voltage of capacity characterising battery concentration polarization in Fig. 5 (b) takes a much longer time to get steady state. In Fig. 5 (c), (d), (e) and (f), the estimated parameters have got to constant values within 4 seconds. Fig. 5 (g) represents the behaviour of estimated voltage and measured voltage of the battery. There is a reasonable

agreement between the estimated voltage and the measured voltage; the maximum estimate error is within 0.3 V, as shown in Fig. 5 (h). This suggests that the extended Kalman filter can be effectively implemented to estimate the parameters of battery model.

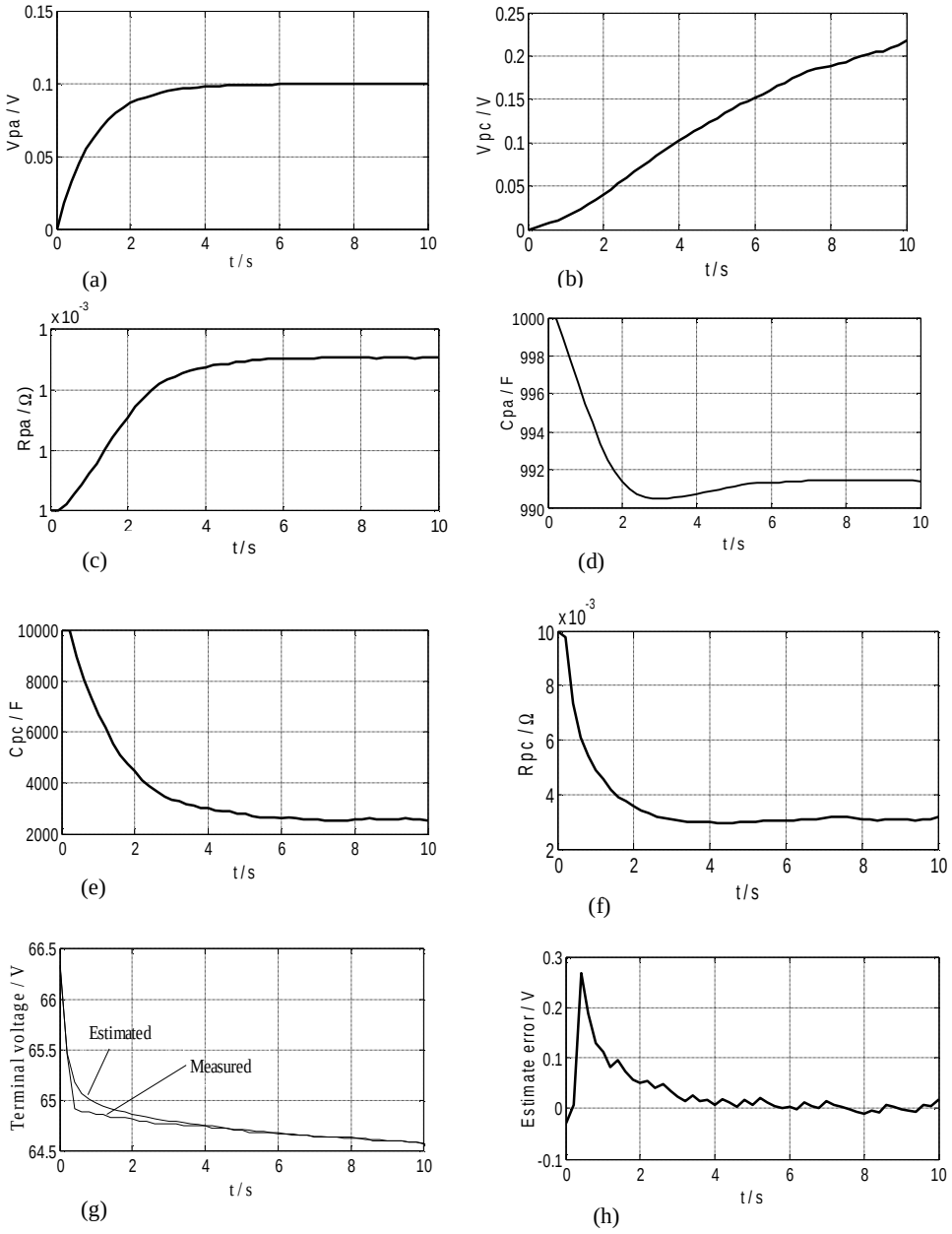

Fig. 5 Estimating results of states and parameters for the battery model with EKF algorithm (SOC=1.0)

4. Simulation and validation

The DST driving cycles [7] was applied for validating the dynamic model of the battery. The initial battery SOC was set to 1.0. The model parameters obtained for a SOC of 1.0, and assumed to be constant during the simulation. This is not strictly true, as the parameter will change with the

change of SOC. But for short operation time, it may be a reasonable approximation. The measured and estimated terminal voltage of the battery is illustrated in Fig. 6. From Fig.6, it is shown that the battery model with the estimated parameters can effectively simulate the battery dynamics, and the battery terminal voltage error shown in Fig. 7 is approximately around 3 %. It is clear that the error will increase with time, and it is necessary to update the parameters to maintain a small error. Fig. 6 suggests that the parameters need to be updated at least every 200 seconds. This will be implemented in the future.

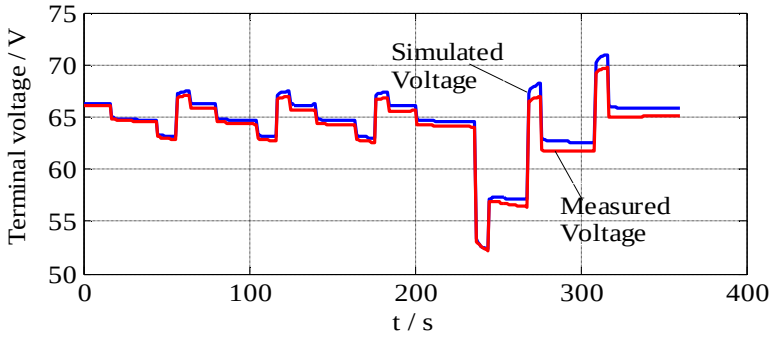

Fig. 6 The simulated and measured voltage of the battery for a DST cycle (SOC_0=0.1)

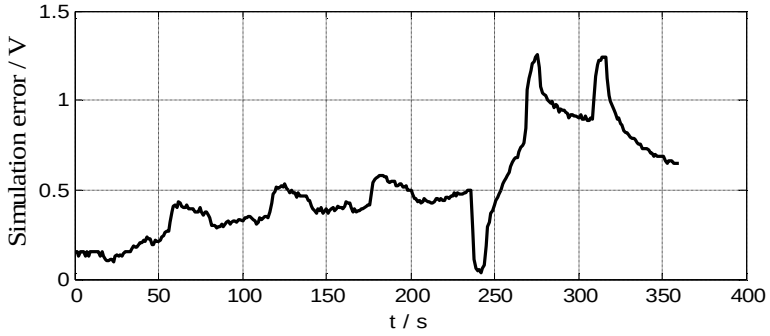

Fig. 7 The simulation error for the battery

5. Conclusions

This paper presented an equivalent circuit model with two RC networks characterising battery activation and concentration polarization process. The extended Kalman filter was used to estimate the coupled parameters reflecting battery polarization characteristics. The parameters characterising battery equilibrium potential and ohmic resistance were determined experimentally. Simulation results using proposed model with the identified parameters, were found to agree satisfactorily with the experimental results. Future work will focus on using EKF to estimate battery states (for example SOC and state of health) and for online model parameters identification.

References

[1] Bumby J R and et al. Computer modelling of the automotive energy requirements for international

combustion engine and battery electric-powered vehicle[C], Proceedings of IEE Pt. A, 1985, 132(5): 265-279.

[2] Glass Michael C. Battery electrochemical nonlinear/dynamic spice model [C]. Energy Conversion Engineering Conference, 1996, pp. 292-297.

[3] O'Gorman C C, Ingersoll D, and F'aez T L. Artificial neural network simulation of battery Performance[C]. IEEE Proceedings of Hawaii International Conference on System Sciences, 1998, pp. 115-121.

[4] CAI Chenghui, DU Dong and et al. Modeling and identification of Ni-MH battery using dynamic neural network[C]. IEEE Proceedings of the First International Conference on Machine Learning and Cybernetics, Beijing, 2002, pp. 1594-1600.

[5] Salameh Z M, Casacca M A and Lynch W A. A mathematical model for lead-acid batteries [J]. IEEE Transactions on Energy Conversions, 1992, 7(1):93-97.

[6] Johnson V H. Battery performance models in ADBISOR [J]. Journal of Power Sources, 2002, 110(8):321-329

[7] IEEEL (Idaho National Engineering & Environmental Laboratory). PNGV Battery Test Manual, Revision 3, DOE/ED-11069, 2003.

[8] Schweighofer B, Raab K M and Brasseur G. Modeling of high power automotive batteries by the use of an automated test system [J]. IEEE Transactions on Instrumentation and Measurement, 2003, 52(4): 1087-1091.

[9] Kroeze R C, Krein P T. Electrical battery model for use in dynamic electric vehicle simulations [C]. IEEE Power Electronics Specialists Conference, 2008, pp. 1336-1342.

[10] Vasebi A, Bathaee S M T and Partovibakhsh M. Predicting State of Charge of Lead-Acid Batteries for Hybrid Electric Vehicles by Extended Kalman Filter [J]. Energy Conversion and Management, 2008, 49(1): 75-82.

[11] Zheng T, McKinnon W R and Dahn J R. Hysteresis during lithium insertion in hydrogen-containing carbons [J]. Journal of Electrochemistry Society, 1996, 143(7):2137-2145.

[12] Inaba M, Fujikawa M, Abe T and Ogumi Z. Calorimetric study on the hysteresis in the charge-discharge profiles of mesocarbon microbeads heat-treated at low temperatures [J]. Journal of Electrochemistry Society, 2000, 147(11):4008-4012.

[13] Murray J J, Sleigh A K and Mckinnon W R. Heats and hysteresis in calorimetry of Li/Li_xMnO_2 cells [J]. Electrochimica Acta, 1991, 36(3-4):489-498.

[14] Sleigh A K, Murray J J and Mckinnon W R. Memory effects due to phase conversion and hysteresis in Li/Li_xMnO_2 cells [J]. Electrochimica Acta, 1991, 36(9):1469-1474.

[15] Welch G, Bishop G. An introduction to the Kalman filter. http://www.cs.unc.edu/~welch/media/pdf/kalman_intro.pdf. Accessed 11 August 2009.

[16] Simon D. Optimal state estimation: Kalman, H infinity, and nonlinear approaches [M]. John Wiley &Sons, 2006.

[17] Dhaouadi R, Mohan N and Norum L. Design and implementation of an extended Kalman filter for the state estimation of a permanent magnet synchronous motor [J]. IEEE Transactions on Power Electrons, 1991, 6(3):491-497.